

Bands, spin fluctuations and traces of Fermi surfaces in angle-resolved photoemission intensities for high- T_C cuprates.

T. Jarlborg

DPMC, University of Geneva, 24 Quai Ernest-Ansermet, CH-1211 Geneva 4, Switzerland

The band structures of pure and hole doped La_2CuO_4 with antiferromagnetic (AFM) spin-fluctuations are calculated and compared to spectral weights of ARPES. It is shown that observations of coexisting Fermi surface (FS) arcs and closed FS pockets are consistent with modulated AFM spin fluctuations of varying wave lengths. Large variations of strong spin fluctuations make the outer part of the FS break diffuse at low doping. This part of the FS is suppressed at high doping when spin fluctuations are weak. The resulting superimposed spectral weight has features both from FS arcs and closed pockets. A connection between results of ARPES, neutron scattering, and band results for the modulated AFM spin wave state, suggests that spin-phonon coupling is an important mechanism for the properties of the cuprates.

PACS numbers: 71.18.+y,74.72.Gh,74.25.Jb,75.30.Fv

I. INTRODUCTION.

The spectral weights of angle-resolved photoemission spectroscopy (ARPES) in moderately hole doped high- T_C cuprates indicate that the Fermi surface (FS) is incomplete, and forms a "FS-arc" that becomes shorter as the temperature is lowered [1–5]. In $\text{Bi}_2\text{Sr}_2\text{CaCu}_2\text{O}_{(8-\delta)}$ the FS is not seen near the the X -point $(\pi, 0)$, which is taken as a signature of an energy gap [6], and a similar behavior in $\text{Ca}_{(2-x)}\text{Na}_x\text{CuO}_2\text{Cl}_2$ has been interpreted as an effect of charge ordering [7]. An incomplete FS would be incompatible with what is known for normal Fermi liquids, since FSs are expected to form closed electron or hole pockets. On the other hand, the ARPES data show sometimes double arcs (like bananas), which are consistent with the existence of closed orbits seen from quantum oscillations in high magnetic field [8]. Oscillations in doped $\text{YBa}_2\text{Cu}_3\text{O}_7$ (YBCO) correspond to a FS area that is much smaller (~ 3 percent) [9] than the area of the large M -centered FS cylinder found in conventional band structure of many cuprates. Unexpectedly, observations of Hall resistance found evidence of electron character for the pocket [10], although it would seem more natural with a hole pocket for that part of the band structure in hole-doped $\text{La}_{(2-x)}\text{Sr}_x\text{CuO}_4$ (LSCO) and YBCO.

Another source of important information about the cuprates has been provided by inelastic neutron scattering, where "hourglass"-shaped (q, ω) -dependences of spin excitations are seen [11–14]. The narrow part with the shortest q -vectors has energies of the same order as the highest phonon energies. Larger q -vectors are found at low energy, and even more so at high energy before the disappearance of spin excitations at even higher $\hbar\omega$. These facts concerning FS features and q -dependence of spin fluctuations seem disconnected, but there might exist a link, which even could be revealing for the mechanisms of superconductivity. While it can be understood that antiferromagnetic (AFM) order can break up a large FS into smaller orbits [15], it is not evident that ARPES should only detect remnants of such orbits at low dop-

ing [5, 16]. It has been argued that smearing due to finite correlation length, ℓ , of the order 10-20 Å (related to lifetime τ of spin fluctuations) leads to effects consistent with observations [15]. In the present work it is shown that also multiple wave lengths of striped spin fluctuations, like in the observations from neutron scattering, lead to an asymmetric FS-smearing. The real-space picture of these fluctuations with vector \vec{q} is that stripe-like potential modulations exist, where $L \approx \pi/q$ is the thickness or wave length of a stripe [17]. The modulations can be static, as suggested for T_C -suppressed 1/8 doped LSCO [18], or more likely dynamic in general cases. Thus, it is suggested that the observation of asymmetric FS-orbits in ARPES is directly connected to multiple q -vectors of spin fluctuations seen in neutron scattering. This provides a clue to the mechanisms of superconductivity, since spin fluctuations with multiple q -excitations are some of the consequences of spin-phonon coupling, SPC. This coupling makes spin waves stronger if they co-exist with phonons of the correct phase and q -vector [19, 20]. The light O-modes are more efficient to enhance the spin waves than the phonons involving heavier elements. Model calculations where the SPC varies with q lead to a spin excitation spectrum quite like what is observed. The effects on the FS from fluctuations with a range of q -vectors as in the SPC model [19] will be tested here.

II. RESULTS AND DISCUSSION.

Different experiments are made for different members of the cuprate family. Some are difficult to cleave into clean surfaces apt for ARPES, and photoemission is mostly made on Bi-based cuprates [1, 3, 5]. Neutron data are taken from large volume samples usually on La based Cu-oxides [11–13], and quantum oscillations were detected in crystals of YBaCuO materials [8]. However, this diversity of systems for the data collection should not hamper an unified understanding of the cuprates, be-

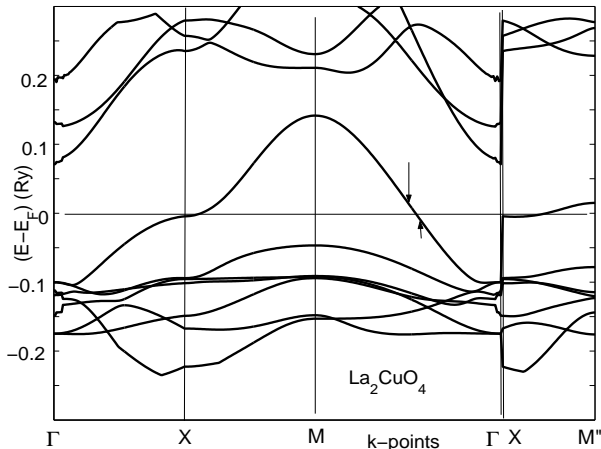


FIG. 1: The bandstructure (nonmagnetic) of La_2CuO_4 for $k_z=0$. AFM order will fold the Brillouin zone, so that the $X-M$ bands are mirrored back on $X-\Gamma$. The bands from M to Γ will be folded at the new zone limit M'' ($\pi/2a_0, \pi/2a_0$), indicated by the downward arrow. When AFM is modulated into stripes the folding moves closer toward Γ (indicated by the upward arrow) and the zone limit at X is reduced correspondingly.

cause their structures and electronic properties are very similar. For instance, almost identical CuO planes are always present, on which AFM moments can appear on Cu , and calculated band structures for different cuprates show the presence of at least one large cylindrical FS ("barrel"). This FS is seen in ARPES, but the intensity is weak for states with k -vectors parallel to the CuO -bond direction, which indicates a gap in this part of the Brillouin zone (BZ). Ultimately, the arc becomes just a point on the diagonal direction at the lowest T [1]. The calculated density-of-state (DOS) at the Fermi energy (E_F) is dominated by the Cu-d electrons from the CuO planes. The present study is based on the band structure of La_2CuO_4 (LCO). The calculations are made using the Linear Muffin-Tin Orbital (LMTO) method and the local spin density approximation. The details of these calculations have been published earlier [21–23]. The nonmagnetic (NM) band structure is shown in Fig. 1. A single barrel-like FS is centered at M (at $\pi/a_0, \pi/a_0$, where a_0 is the in-plane lattice constant). AFM order on the Cu lattice will double the unit cell, and the bands are split by exchange and folded into a half as big AFM BZ. This can be followed by comparing the original bands in Fig. 1 with the bands calculated for the AFM cell shown in Fig. 2 within the AFM BZ. It can be noted that the exchange splitting, ξ , is largest near E_F (on the $X-M''$ line) while it is lower below E_F . The original barrel is fragmented into two pieces by AFM. One banana-like feature at M'' (which might look like an arc if it is narrow), and another rounded piece at X . The latter is delicate by two reasons. First, the band is very flat (a heavy effective mass) at X , which makes the FS sensitive to disorder and fluctuations. Secondly, it disappears at high hole

doping when E_F is lower. It does not have a dispersive band as the other piece has from M'' to Γ , see Fig. 2. A dispersive band has a sharp FS break which is easy to detect in photoemission. But at the end points of the banana, between M'' and X , the band is flat and the FS break is diffuse. An insulating gap will be opened at E_F for increased exchange splitting, when both the hole pocket at M'' and the electron pocket at X disappear. However, the X pocket is the first to disappear because of hole doping and a low E_F . Such cases are considered in the present model calculations.

The AFM order on Cu neighbors separated by a distance a_0 (wave vector $\vec{Q} = \pi/a_0$) can be modeled by a nearly free electron (NFE) potential perturbation $V(x) = \xi_0 \exp(i\vec{x} \cdot \vec{Q})$, where ξ_0 is the maximum of the exchange splitting [22]. The potential for a stripe modulation with period $N \cdot a_0$ (wave vector $q = \vec{Q}/N$) is obtained by multiplying the potential by $\exp(-i\vec{x} \cdot \vec{q})$. Totally this gives

$$V(x) = \xi_0 e^{i\vec{x} \cdot (\vec{Q} - \vec{q})} \quad (1)$$

and the zone boundary will regress from π/a_0 to $\pi(1 - 1/N)/a_0$. The gap in a NFE model based on this potential will follow the zone boundary, and the gap moves down in energy when \vec{q} increases [17, 22]. Ab-initio band calculations confirm that the gap moves toward lower energy when the modulation is made within longer and longer unit cells, and the pseudogap at E_F is a result of the striped modulations [21, 23]. By folding the bands of Fig. 1 it is possible to reconstruct the AFM bands, like the ones in Fig. 2. Plots of the FS are made by tracking k -points with $|E(k) - E_F| < 2mRy$ within a BZ of 100 by 100 k -points in the $k_z = 0$ plane. The reconstructed FS orbits are displayed in Fig. 3, where one case with modulated AFM is shown by the displaced orbit. Effects of finite τ or spread of modulated q -vectors are not yet included, and therefore, both sides of the FS are equally sharp.

The effect of finite correlation length for quasistatic AFM modulations and τ has been shown to make an asymmetric smearing of ARPES intensities [15]. The result on the FS is similar in the present work, but the origin is here directly connected to the observed spin wave excitations. A distribution of q -vectors makes the smearing different on the inner (toward Γ) and outer FS break. Different q -vectors can be characteristic for different domains in the material, where local variations of the doping make the spin fluctuations weak or strong. Such domains might very well be larger than the typical correlation length, and here it is the q -value and not the correlation length that determines the broadening. Emitted electrons in ARPES come from a wide area compared to the size of the domains, and an average of the different \vec{q} from the domains will be detected. Life-time broadening will not contribute for static domains. Or more likely, if fluctuations of different \vec{q} are continuously mixed in space and time, there will be additional smearing from τ , since the life-time of the electronic states is

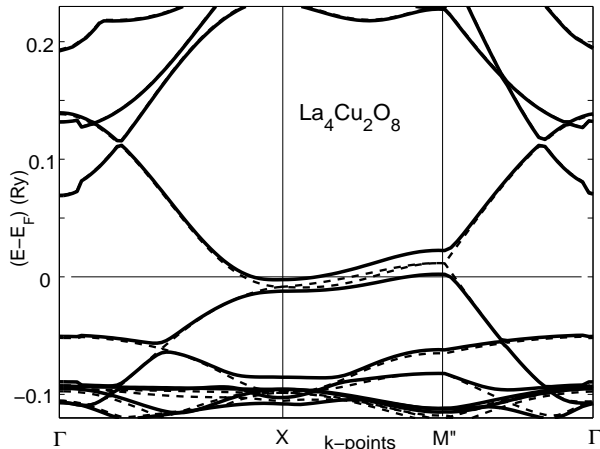


FIG. 2: The bandstructure of nonmagnetic (broken lines) and AFM (full lines) $\text{La}_4\text{Cu}_2\text{O}_8$ in the AFM Brillouin zone for $k_z=0$. The AFM configuration is obtained by having a staggered magnetic field on Cu (± 7 mRy). The moments are $\pm 0.19 \mu_B/\text{Cu}$.

shortened. The present model will not distinguish between these two possibilities since effects of multiple \vec{q} exist static and dynamic spin waves. Other effects such as diffusion at impurities and phonons will shorten τ and make all parts of the FS diffuse. The effects of multiple q are very different on the inner and outer FS branches, such as seen experimentally. Thus, together with the expected doping dependence, it is possible to separate standard FS broadening effects from q -wave effects.

Neutron scattering has shown that the q -vectors of spin excitations vary from 0.05 (π/a_0 units) at intermediate energy to 0.15 at low energy or even 0.2 for energies clearly above phonon energies [11]. However, the intensity decreases rapidly above 60 meV, so spin fluctuations are mainly found for $\hbar\omega$ in the range of phonon energies. Furthermore, all q -values decrease at lower doping [12]. Such behaviors agree with models of spin-phonon coupling, where strong spin fluctuations coupled to oxygen phonon modes lead to small q -vectors and vice-versa for interaction with low frequency modes [19]. Within the range $\hbar\omega \sim 10$ - 60 meV and $\vec{q} \sim 0.05$ - 0.15 , the amplitudes of ξ_0 are 20 - 30 mRy in the model for spin-phonon coupling. Hence, the q -vectors can vary a factor of 3, when the exchange splitting varies ± 20 percent, and the effect of smearing coming from exchange shifts of the band is rather small in comparison to smearing from q -variations.

The inner part of the FS (the one closest to Γ) can only be smeared if there are variations of ξ . But as the variation of ξ within the band is rather small, and ξ becomes smaller further away from E_F , it leads only to small broadening effects of the inner band. On the other hand, the FS crossing of the outer part can be shifted much more depending on how the band is reflected in a multitude of zone boundaries. This is sketched in Fig. 4, where the heavy full (nonmagnetic) and broken (exchange splitted) lines show the band dispersion in the

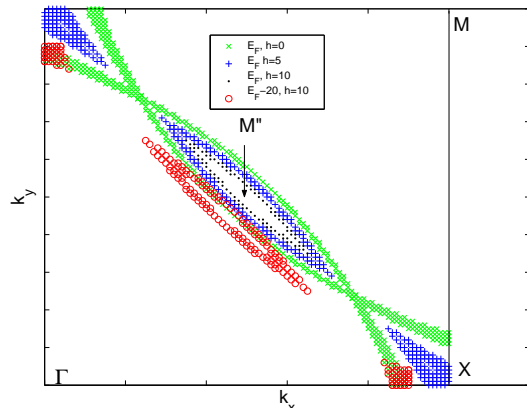


FIG. 3: (Color online) The evolution of the AFM FS for increased exchange splitting ($h=0, 5, 10, 20$ mRy) are shown by green "x", blue "+" and black ".", respectively. The original "unfolded" FS for $h=0$ has only one circular FS centered around the M -point ($\pi/a_0, \pi/a_0$). Two disconnected FS are formed when h increases. One at X , which is diffuse and disappears at high doping, and one at M'' with clear FS breaks toward Γ and M . This piece of FS is displaced toward Γ when AFM is q -modulated into stripes (red "o").

AFM zone near M'' on a line of k -points going from the zone center in the 2nd BZ (i.e. M in the normal BZ) toward Γ . When disorder in form of three modulated stripes with new reduced zone boundaries are introduced, and ξ is constant, there will be three FS crossings on the outside part of the FS, while the FS break remains sharp in the direction of Γ . This effect of smearings on the inner and outer sides of the FS is attenuated if ξ decreases with increasing q , but as was mentioned, effects from the estimated variation of ξ are small in comparison to variations of q .

An average of the FS signal is made from a set of about 20 equally spaced q -vectors. The bands in Fig. 1 are folded into the zones of increasing q . The range of q - and ξ -values is a factor of 3 and ± 20 percent, respectively, as was concluded above. Fig. 5 shows an example with the $\xi = 12.5 \pm 2.5$ mRy and q in the range $[0.012-0.04]$. At these conditions a trace of the outermost FS remains near M'' , with a minimum of the intensity closer to Γ , between the inner and outer FS-parts, similar to what was observed by Meng *et al* for underdoped Bi-2201 [5]. The main inner peak is even more dominant when spin fluctuations are weak or absent. This is because at weaker spin fluctuations there are larger q and larger relative spread Δq which contribute to a diffuse outer part of the FS. (Oppositely, $q \rightarrow 0$ if only strong fluctuations are present so that also $\Delta q \rightarrow 0$.) This situation is approached in Fig. 6. Smaller ξ implies larger \vec{q} , and the widths of q -values make stronger smearing of the outer branch, and no minimum is seen between the two FS branches in Fig. 6. The main inner peak appears slightly closer toward Γ in Fig. 6 than in Fig. 5, because of the general expansion of the FS barrel for increased hole doping. The

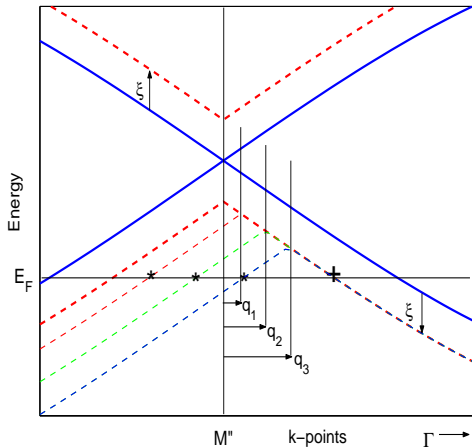


FIG. 4: (Color online) A schematic close-up of the bands near the M'' -point. The non-spinpolarized band is reflected at the zone boundary at M'' to create the band structure for weak AFM (full lines). An exchange energy ξ will split the bands (heavy broken lines) and displace the FS-breaks closer to M'' . The bands from 3 striped AFM waves, modulated with 3 different q -vectors (q_1, q_2 and q_3), will be reflected by the 3 new zone limits indicated by the short vertical lines, as described in the text. These bands (thin broken lines) make FS crossings at different positions (*) on the part outside the zone limits, while they are all superimposed on one FS crossing (+) on inside part, i.e. the part closest to Γ .

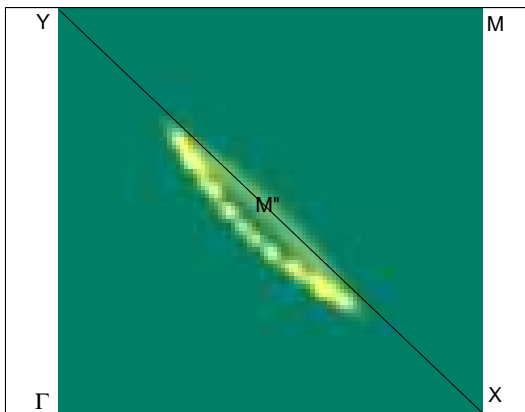


FIG. 5: (Color online) An intensity plot (the occurrence of having the bands within 2 mRy of E_F for each k_x, k_y -bin) for the folded FS of LCO with E_F shifted to be close to optimal doping. The exchange is 10-15 mRy with q from 0.04 to 0.012.

central region for maximum intensity from the outer FS happens to be near M'' in Figs. 5 and 6, but there is no fundamental reason for this. Remnants of the outer FS are identified near or slightly inside the M'' positions in ARPES for two underdoped compositions of Bi2201, and a very broad and unstructured distribution has been observed for optimal doping [5]. Finally, if $\xi \rightarrow 0$ then the non-magnetic (unfolded) BZ is appropriate with only the inner FS branch.

Spin fluctuations are strong at low doping before static

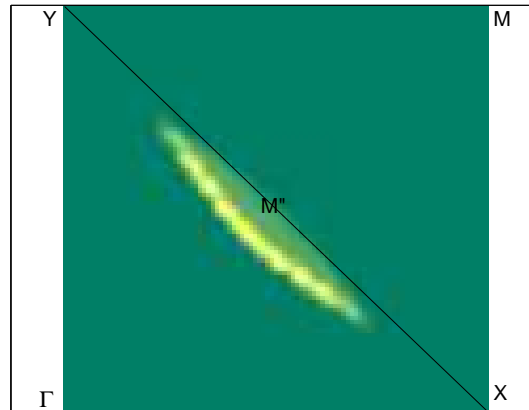


FIG. 6: (Color online) As in Fig. 5, but for 3 mRy lower E_F , with ξ 8-12 mRy and q 0.08-0.03.

AFM order occurs in undoped insulating cuprates. On the contrary, at high doping it is believed that fluctuations and ξ decrease to a point when a representation of the FS within the NM BZ becomes appropriate. Of course, only the inner branch of the FS exists for the NM case. The inner FS part from weak fluctuations will overlap with the single FS of the NM FS, while the outer part from weak fluctuations will be faint and broad. Therefore, the observation in ref. [5] for the highest doping might be a case toward weakened striped fluctuations with a dominant signal from the NM FS.

The independent work of Harrison *et al* [15] relies on a model of Lee *et al* [24] for a Lorentzian probability distribution for the diffusion, where wave vectors and a spin correlation length ℓ are parameters. By deviating the wave vector from the zone limit they obtain a displacement of the FS orbit, as in the present work. The extreme limits of their FS smearing is introduced by varying ℓ from 100 to 5 Å. The similarity of the two approaches is evident for the q -dependence, while in the present work smearing is introduced by the step-like range of q -vectors. An estimate of the correlation length is not directly comparable with ℓ in ref [15], because of the different distributions and cut-offs in real and reciprocal space, but if $\ell \approx L \approx \pi/\Delta q$ and Δq are 0.028 and 0.05 in Figs. 5 and 6, we can deduce correlation lengths of roughly 120-60 Å as an order of magnitude of the lengths in these two cases. Harrison *et al* derived damping properties for quantum oscillation from these parametrized calculations for different correlation lengths. A corresponding analysis will not be undertaken here, but because of the similarities of the two approaches it can be assumed that the damping properties of quantum oscillation will be close to the results of ref [15] for rather large ℓ .

The present model includes a uniform distribution of fluctuations within the (q, ξ) -interval, with no contributions outside. For instance, Fig. 6 is based on 16 equally spaced (q, ξ) -values starting from (0.03,12) and ending at (0.08,8) (in units of *r.l.u* and *mRy*), see Fig. 7. Real fluctuations from O-modes with $\hbar\omega$ around 50 meV con-

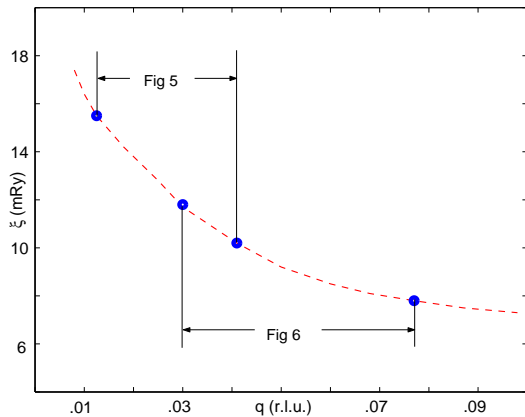


FIG. 7: (Color online) Approximate ranges of the exchange splitting, ξ , as function of modulation vector, q , used for Figures 5 and 6.

tribute mostly to the low- q , high- ξ part of the ranges (to the left in Fig. 7) [19], and such particular (q, ξ) -values would show increased intensity in neutron data [11–14]. Such variations could modify the details of the appearance of ARPES intensities [25], but the extreme case with only one (q, ξ) -value would make the breaks of the inner and outer parts of the FS equally sharp. However, possible effects of limited correlation lengths remain. The (q, ξ) -range in Fig. 7 will, according to the model for spin-phonon coupling, move more to the right and be wider if the hole-doping increases [19, 23].

Finally, a comment about the charge character of the small M'' centered orbit. From Fig. 2 it appears to be hole like when the pocket is very small. However, the charge character depends on the curvature of the band ϵ_k , i.e. $d^2\epsilon_k/dk^2$ [26]. As is seen in Fig. 2 between X and M'' there is an increasingly positive second derivative of

the band when E_F gets lower from hole doping, which is a signature of electronic character. The band is rather flat in this portion of the FS, so it contributes significantly to the DOS and it may explain the unexpected electron-like character of the band in Hall measurements [10]. If so, from the dispersion of the band in Fig. 2 it can be expected that the electron character gets weaker for less hole doping, i.e. when the area of the orbit becomes very small. An alternative explanation is that rests of the X-pocket are contributing even at intermediate doping [10].

III. CONCLUSION

The FS of a hole doped AFM cuprate has a banana shaped hole pocket centered slightly inside the M'' -point. In addition to effects from the finite correlation length of spin fluctuations [15], it is shown here that stripe-like modulations of spin fluctuations with multiple q -values make the outer part of this FS diffuse, while the inner part remains sharp. Only the latter part is visible for weak or nonexistent spin fluctuations. A distribution of different exchange splittings is important for asymmetric broadening through the connection to variations of q . Both lifetime broadening and static fluctuations of different strengths within domains lead to asymmetric broadening. A natural connection between results of ARPES [1, 3, 5] and neutron scattering [11–14] is suggested. Furthermore, spin-phonon coupling has been shown to be compatible with the (q, ω) -dependence of spin excitations, and it might be an important ingredient for the mechanisms behind pseudogaps and superconductivity [19]. A concordance between ARPES intensities and spin excitations seen by neutrons indicates that spin-phonon coupling is at work in the cuprates.

-
- [1] M.R. Norman, H. Ding, M. Randeria, J.C. Campuzano, T. Yokoya, T. Takeuchi, T. Takahashi, T. Mochiku, K. Kadowaki, P. Guptasarma and D.G. Hinks, *Nature (London)* **392**, 157 (1998).
- [2] A. Kanigel, M.R. Norman, M. Randeria, U. Chatterjee, S. Souma, A. Kaminski, H.M. Fretwell, S. Rosenkranz, M. Shi, T. Sato, T. Takahashi, Z.Z. Li, H. Raffy, K. Kadowaki, D. Hinks, L. Ozyuzer and J.C. Campuzano, *Nat. Phys.* **2**, 447, (2006).
- [3] A. Damascelli, Z.-X. Shen and Z. Hussain, *Rev. Mod. Phys.* **75**, 473, (2003).
- [4] J. Hwang, J.P. Carbotte and T. Timusk, *Eur. Phys. Lett.* **82**, 27002, (2008).
- [5] J. Meng, G. Liu, W. Zhang, L. Zhao, H. Liu, X. Jia, D. Mu, S. Liu, X. Dong, J. Zhang, W. Lu, G. Wang, Y. Zhou, Y. Zhu, X. Wang, Z. Xu, C. Chen and X. Zhou, *Nature (London)* **462**, 335 (2009).
- [6] D.S. Marshall, D.S. Dessau, A.G. Loeser, C-H. Park, A.Y. Matsuura, J.N. Eckstein, I. Bozovic, P. Fournier, A. Kapitulnik, W. E. Spicer, and Z.-X. Shen, *Phys. Rev. Lett.* **76**, 4841 (1996).
- [7] K.M. Shen, F. Ronning, D.H. Lu, F. Baumberger, N.J.C. Ingle, W.S. Lee, W. Meevasana, Y. Kohsaka, M. Azuma, M. Takano, H. Takagi and Z.-X. Shen, *Science* **307**, 901, (2005).
- [8] E.A. Yelland, J. Singleton, C.H. Mielke, N. Harrison, F.F. Balakirev, B. Dabrowski and J.R. Cooper, *Phys. Rev. Lett.* **100**, 047003, (2008).
- [9] N. Doiron-Leyraud, C. Proust, D. LeBoeuf, J. Levallois, J.-P. Bonnemaison, R. Liang, D.A. Bonn, W.N. Hardy and L. Taillefer, *Nature (London)* **447**, 565, (2007).
- [10] D. LeBoeuf, N. Doiron-Leyraud, J. Levallois, R. Daou, J.-P. Bonnemaison, N.E. Hussey, L. Balicas, B.J. Ramshaw, R. Liang, D.A. Bonn, W.N. Hardy, S. Adachi, C. Proust and L. Taillefer, *Nature (London)* **450**, 533, (2007).
- [11] B. Vignolle, S.M. Hayden, D.F. McMorrow, H.M. Rönnow, B. Lake and T.G. Perring, *Nat. Phys.* **3**, 163, (2007).
- [12] J.M. Tranquada, H. Woo, T.G. Perring, H. Goka, G.D. Gu, G. Xu, M. Fujita and K. Yamada, *Nature (London)*

- 429**, 534 (2004).
- [13] M. Matsuda, M. Fujita, S. Wakimoto, J.A. Fernandez-Baca, J.M. Tranquada and K. Yamada, Phys. Rev. Lett. **101**, 197001, (2008).
- [14] V. Hinkov, P. Bourges, S. Pailhès, Y. Sidis, A. Ivanov, C.D. Frost, T.G. Perring, C.T. Lin, D.P. Chen and B. Keimer, Nat. Phys. **3**, 780, (2007).
- [15] N. Harrison, R.D. McDonald and J. Singleton, Phys. Rev. Lett. **99**, 206406, (2007).
- [16] P.D.C. King, J.A. Rosen, W. Meevasana, A. Tamai, E. Rozbicki, R. Comin, G. Levy, D. Fournier, Y. Yoshida, H. Eisaki, K.M. Shen, N.J.C. Ingle, A. Damascelli, and F. Baumberger, Phys. Rev. Lett. **106**, 127005, (2011).
- [17] T. Jarlborg, Adv. Cond. Matt. Phys., **2010**, 912067 (2010).
- [18] A.R. Moodenbaugh, Y. Xu, M. Suenaga, T. J. Folkerts and R. N. Shelton, Phys. Rev. B **38**, 4596 (1988).
- [19] T. Jarlborg, Phys. Rev. **B79**, 094530, (2009).
- [20] P. Piekarczyk and T. Egami, Phys. Rev. **B72**, 054530, (2005).
- [21] T. Jarlborg, Phys. Rev. **B64**, 060507(R), (2001).
- [22] T. Jarlborg, Phys. Rev. **B76**, 140504(R), (2007).
- [23] T. Jarlborg, Physica **C454**, 5, (2007).
- [24] P.A. Lee, T.M. Rice, and P.W. Anderson, Phys. Rev. Lett. **31**, 462, (1973).
- [25] Grouping of q-vectors around particular values will be favorable for quantum oscillations because of smaller effective Δq .
- [26] P.B. Allen, W.E. Pickett, and H. Krakauer, Phys. Rev. **B37**, 7482 (1988).